CDF note 8140

Measurement of B Hadron Relative Fragmentation Fractions

The CDF Collaboration
URL http://www-cdf.fnal.gov
(Dated: March 28, 2006)

This note describes the first Run II measurement of b quark fragmentation into $\bar{B}^0$, B^-, $\bar{B}_s^0$ and Λ_b^0 using semileptonic B decays reconstructed in 360 pb^{-1} of data taken with the ℓ+SVT triggers. The fragmentation fractions are measured for an effective B hadron p_T threshold of 7 GeV/c to be $f_u/f_d = 1.054 \pm 0.018(stat)^{+0.025}_{-0.045}(sys) \pm 0.082(\mathcal{BR})$, $f_s/(f_u + f_d) = 0.160 \pm 0.005(stat)^{+0.011}_{-0.010}(sys)$ $^{+0.057}_{-0.034}(\mathcal{BR})$, and $f_{\Lambda_b}/(f_u + f_d) = 0.281 \pm 0.012(stat)^{+0.058}_{-0.056}(sys)^{+0.128}_{-0.086}(\mathcal{BR})$.

Preliminary Results for Spring 2006 Conferences

I. INTRODUCTION

Bottom quarks produced in hadronic collisions combine with quarks and gluons to form a hadron. In this process, called fragmentation, the color force field creates additional quark-antiquark pairs that combine with the bottom quark to create a b flavored hadron: a B meson or b baryon. The fragmentation process is governed by the strong force and cannot be reliably calculated by perturbative QCD. Therefore, the fragmentation properties of b quarks must be determined empirically. This note described the measurement of the flavor dependence of the fragmentation process for b quarks produced in hadronic $p\bar{p}$ collisions at $\sqrt{s} = 1.96$ TeV. The probabilities that the fragmentation of a $\bar{b}$ quark will result in a B^-, $\bar{B}^0$, $\bar{B}^0_s$ meson and Λ^0_b baryon are defined as f_u, f_d, f_s and f_{Λ_b} respectively [1]. The contributions from the production of excited B hadrons that decay into final states containing a B^-, $\bar{B}^0$, $\bar{B}^0_s$ meson or Λ^0_b baryon are explicitly included in this definition of the fragmentation fractions. In order to reduce systematic uncertainties arising from the poor knowledge of the b quark production cross section or absolute determinations of trigger or tracking efficiencies, the b quark fragmentation fractions are measured relative to f_d.

In Run I of the Fermilab Tevatron, the fraction of $\bar{B}^0_s$ mesons produced relative to the number of $\bar{B}^0$ mesons was measured $\sim 2\sigma$ higher at CDF [2] than at the LEP experiments [3]. To shed light on the question of whether b quark fragmentation could be different in a hadron environment than in e^+e^- collisions, the measurement of the fragmentation fractions in CDF Run II is clearly of interest. Previously, B fragmentation fractions have been quoted as absolute fractions independent of kinematic quantities such as $p_T(B)$ [2]-[5]. In this text f_q indicates the fragmentation fraction integrated above the p_T threshold of sensitivity; $f_q \equiv f_q(p_T(B) \ > \ 7.0 \ GeV/c)$.

II. DATA SAMPLE

The data used in this analysis represents an integrated luminosity of approximately 360 pb^{-1} collected with the CDF II detector between February 2002, and August 2004. The CDF detector is described in detail elsewhere [6]. Semileptonic decays of B hadrons provide large statistics samples for studying the fragmentation properties of b quarks. This measurement uses both the μ and e plus displaced track (SVT) triggers, which requires the $p_T(\ell) > 4$ GeV/c, p_T(SVT track) > 2 GeV/c, and 120 μm $\geq d_0 \leq 1$ mm, where d_0 is the SVT track impact parameter. The displaced track is required to be one of the tracks in the five charm signals which are reconstructed: $D^0 \to K^-\pi^+$, $D^{*+} \to D^0\pi^+$, $D^+ \to K^-\pi^+\pi^+$, $D^+_s \to \phi(\to K^+K^-)\pi^+$, and $\Lambda^+_c \to pK^-\pi^+$, shown in Figure 1 for the μ+SVT data and in Figure 2 for the e+SVT data. These reconstructed charm signals are vertexed with the triggered lepton to establish signals which can be related to semileptonic B^-, $\bar{B}^0$, $\bar{B}^0_s$, and Λ^0_b decays. The reflection of D^+_s decays into the D^+ final state due to $K-\pi$ mis-identification is included in the fit to the D^+ signal. The large combinatorial and reflection backgrounds in the Λ^+_c signal, shown in Figure 3, is reduced by making a cut on the dE/dx likelihood ratio $\mathcal{LR} \equiv \mathcal{L}(p)/[\mathcal{L}(p) + \mathcal{L}(K) + \mathcal{L}(\pi) + \mathcal{L}(e) + \mathcal{L}(\mu)] > 0.3$, shown in Figure 4. The final lepton-charm yields are listed in Table I.

Signature	e+SVT Yield	μ+SVT Yield
$\ell^- D^0$	16,939±160	29,909±224
$\ell^- D^{*+}$	2,998±56	5,492±77
$\ell^- D^+$	10,779±149	20,236±216
$\ell^- D^+_s$	1,012±44	2,069±84
$\ell^- \Lambda^+_c$	1,755±106	2,984±130

TABLE I: Signal yields for lepton-charm final states in 360 pb^{-1}.

III. SAMPLE COMPOSITION

This analysis makes use of the spectator model describing semileptonic B meson decays, which predicts that the partial width of the semileptonic decays of B mesons are equal:

$$\Gamma(\bar{B}^0 \to \ell^-\bar{\nu}_\ell X) = \Gamma(B^- \to \ell^-\bar{\nu}_\ell X) = \Gamma(\bar{B}^0_s \to \ell^-\bar{\nu}_\ell X), \tag{1}$$

where

$$\Gamma(B \to \ell\nu D^{(*,**)}) = \frac{1}{\tau(B)}\mathcal{BR}(B \to \ell\nu D^{(*,**)}). \tag{2}$$

From the spectator model, the partial widths of the semileptonic B decays into the pseudoscalar, vector, or higher excited D states are expected to be equal. For example, we assume

$$\Gamma(\bar{B}^0 \to \ell^-\bar{\nu}_\ell D^+) = \Gamma(B^- \to \ell^-\bar{\nu}_\ell D^0) = \Gamma(\bar{B}^0_s \to \ell^-\bar{\nu}_\ell D^+_s) = \Gamma(B \to \ell\nu D), \tag{3}$$

with similar relations for D^* and D^{**} decays. The additional constraint that

$$\Gamma(\bar{B} \to \ell\bar{\nu}_\ell D) + \Gamma^*(\bar{B} \to \ell\bar{\nu}_\ell D^*) + \Gamma^{**}(\bar{B} \to \ell\bar{\nu}_\ell D^{**}) = \Gamma(\bar{B} \to \ell\bar{\nu}_\ell X) \tag{4}$$

is also applied to the partial widths. This constraint includes in the D^{**} partial width all other semileptonic decays besides D and D^*, such as nonresonant decays in addition to actual D^{**} decays. Since the Λ_b baryon is not necessarily well-described by the spectator model, fixed branching ratios are used to describe the Λ_b^0 semileptonic decays.

If the only source of $\ell^- D^+$ combinations were from the direct decay of a neutral B meson $\bar{B}^0 \to \ell^-\nu D^+$, the number of reconstructed $\ell^- D^+$ events can be determined as follows:

$$N(\ell^- D^+) = N(\bar{B}^0) \times \mathcal{BR}(\bar{B}^0 \to \ell^-\bar{\nu}_\ell D^+) \times \mathcal{BR}(D^+ \to K^-\pi^+\pi^+) \times \epsilon(\bar{B}^0 \to \ell^-\bar{\nu}_\ell D^+) \tag{5}$$

where $N(\bar{B}^0)$ represents the numbers of produced $\bar{B}^0$ mesons. However, cross-talk between the various B hadron species via the excited charm states necessitates a sample composition parameterization to relate the lepton-charm signals to the parent B hadrons. Introducing the relative fragmentation fractions, the sample composition for the $\bar{B}^0$ can be written (for illustrative purposes) as:

$$\begin{aligned} N(\ell^- D^+) = {} & N(\bar{B}^0)\mathcal{BR}(D^+ \to K^-\pi^+\pi^+) \\ & \times \Bigg[\sum_{\bar{B}^0 \to D^+ X} \mathcal{BR}(\bar{B}^0 \to \ell^-\bar{\nu}_\ell D^+ X)\epsilon(\bar{B}^0 \to \ell^-\bar{\nu}_\ell D^+ X) \\ & + \frac{f_u}{f_d} \sum_{B^- \to D^+ X} \mathcal{BR}(B^- \to \ell^-\bar{\nu}_\ell D^+ X)\epsilon(B^- \to \ell^-\bar{\nu}_\ell D^+ X) \\ & + \frac{f_s}{f_u + f_d}\left(1 + \frac{f_u}{f_d}\right) \sum_{\bar{B}^0_s \to D^+ X} \mathcal{BR}(\bar{B}^0_s \to \ell^-\bar{\nu}_\ell D^+ X)\epsilon(\bar{B}^0_s \to \ell^-\bar{\nu}_\ell D^+ X) \Bigg] \end{aligned} \tag{6}$$

The sample composition requires knowledge of the branching ratios of the charm hadrons, which are determined from the PDG [5] when available and from the `EvtGen` decay package predictions [7] when not available in the PDG, and the efficiency of the decay, which is determined from Monte Carlo simulation. In addition to the primary decays which contribute to the semileptonic signal, indirect semileptonic decays (*e.g.* $B \to DD$) are also included in the sample composition. All of the decays considered in the B hadron sample composition are listed in Appendix A.

The bottom meson branching ratios are included via the partial widths, listed in Table II, and adjusted by the lifetime of the B hadron, given in Table III. The branching ratios used for the Λ_b^0 semileptonic decays are estimated from measurements of the branching ratios made in other CDF measurements [8] (c.f. Table IV). The ground state charm branching ratios used in the analysis are listed in Table V.

B Decay	Width ($\times 10^{-12}$ ps^{-1})
$\Gamma(B \to \ell\nu D)$	0.0134±0.0009
$\Gamma^*(B \to \ell\nu D^*)$	0.0372±0.0017
$\Gamma^{**}(B \to \ell\nu D^{**})$	0.0141±0.0010

TABLE II: Partial widths of the B mesons used.

IV. EFFICIENCIES

Many efficiencies in the measurement of the relative fragmentation fractions are expected to cancel. Many of the remaining relative efficiencies are determined from Monte Carlo simulation. A few efficiencies which are not well described by Monte Carlo are instead determined from the data:

- Differences in the first level eXtremely Fast Tracker (XFT) trigger efficiencies of kaons, pions, and protons. These efficiencies are binned in run ranges spanning the data set used, shown in Figure 5 for the K and π efficiencies in data and in Figure 6 for the efficiencies of the data relative to the Monte Carlo for K and π

B Lifetimes	[ps]
$\tau(B^0)$	1.536±0.014
$\tau(B^-)$	1.671±0.018
$\tau(B^-)/\tau(\bar{B}^0)$	1.086±0.017
$\tau(\bar{B}_s^0)$	1.461±0.057
$\tau(\Lambda_b^0)$	1.229±0.080

TABLE III: B hadron lifetimes used in the measurement.

Λ_b^0 Decay	$\mathcal{BR}$
$\ell^-\bar{\nu}_\ell\Lambda_c^+X$	(9.2±2.1)%
$\ell^-\bar{\nu}_\ell\Lambda_c^+$	(6.54±0.22)%
$\ell^-\bar{\nu}_\ell\Lambda_c(2593)^+$	$(3.07\pm1.02)\times10^{-3}$
$\ell^-\bar{\nu}_\ell\Lambda_c(2625)^+$	$(5.14\pm0.99)\times10^{-3}$
$\ell^-\bar{\nu}_\ell\Sigma_c(2455)^{++}\pi^-$	$(2.7\pm1.0)\times10^{-3}$
$\ell^-\bar{\nu}_\ell\Sigma_c(2455)^{+}\pi^0$	$(2.7\pm1.0)\times10^{-3}$
$\ell^-\bar{\nu}_\ell\Sigma_c(2455)^{0}\pi^+$	$(2.7\pm1.0)\times10^{-3}$
$\ell^-\bar{\nu}_\ell\Lambda_c f_0$	$(2.6\pm??)\times10^{-3}$
$\ell^-\bar{\nu}_\ell\Lambda_c\pi^+\pi^-$ (NR)	$(5.2\pm??)\times10^{-3}$
$\ell^-\bar{\nu}_\ell\Lambda_c\pi^0\pi^0$ (NR)	$(2.6\pm??)\times10^{-3}$

TABLE IV: Λ_b^0 branching ratios used in the measurement.

- The efficiency of the dE/dx cut which has been applied to the proton in the $\Lambda_c^+ \to pK^-\pi^+$ decay, shown in Figure 4 for the different particle species.
- The difference in efficiency due to a two track charm topology instead of a three track topology arising from the efficiency to add a single track to a decay. This efficiency has been measured to be $\epsilon_{trk} = 87.8\pm0.8(stat)^{+1.9}_{-0.9}(sys)\%$.

The relative efficiencies included in the sample composition are the product of the acceptance, trigger, and analysis efficiencies,

$$\begin{aligned}\epsilon_{rel}(\ell^-D^+) &= \epsilon_{acceptance}(MC)\times\epsilon_{trigger}(MC)\times\epsilon_{analysis}(MC)\\ &\quad\times\epsilon_{p/K/\pi\ trigger}(Data/MC).\end{aligned} \tag{7}$$

where the efficiencies are similar for the other lepton-charm signals. An extra factor of $\epsilon^{-1}_{singletrack}(Data/MC)$ is needed for $\epsilon_{rel}(\ell^-D^0)$ and $\epsilon_{rel}(\ell^-D^{*+})$ to adjust the two track charm topology relative to the three track charm states, while the $\ell^-\Lambda_c^+$ relative efficiency requires an additional efficiency, $\epsilon_{dE/dx}(Data)$, for the dE/dx cut on the proton.

V. FIT

A χ^2 fit is used to extract the fragmentation fractions from the sample composition. The measured yields in the five lepton-charm signals are fit to the yields predicted by the sample composition and the decay rates ($\Gamma^{(*,**)}$) of the

Charm Decay	$\mathcal{BR}(\%)$
$D^+ \to K^-\pi^+\pi^+$	8.8±0.6
$D^0 \to K^-\pi^+$	3.80±0.09
$D^{*+} \to D^0\pi^+$	67.7±0.5
$D_s^+ \to \phi\pi^+$	3.6±0.9
$\phi \to K^+K^-$	49.1±0.6
$\Lambda_c^+ \to pK^+\pi^-$	5.0±1.3

TABLE V: Ground state charm branching ratios used in the measurement.

B meson to the ground and excited states are constrained within their errors. The χ^2 which is minimized is

$$\chi^2 = \sum_{i=1}^{5} \left(\frac{N_i(\ell + charm)_{measured} - N_i(\ell + charm)_{predicted}}{\sigma_{N_{i,measured}}} \right)^2 + \left(\frac{\Gamma - \Gamma_{PDG}}{\sigma_{\Gamma_{PDG}}} \right)^2 + \left(\frac{\Gamma^* - \Gamma^*_{PDG}}{\sigma_{\Gamma^*_{PDG}}} \right)^2 + \left(\frac{\Gamma^{**} - \Gamma^{**}_{PDG}}{\sigma_{\Gamma^{**}_{PDG}}} \right)^2 . \quad (8)$$

$N_{predicted}$ is determined from the sample composition and $N_{measured}$ is determined from the data. In order to simplify the sample composition in the fit and also to fit in terms of better known quantities, the number of predicted lepton-charm events are expressed in terms of $N(\bar{B}^0)$, which is an overall normalization in the fit and not indicative of the physical number of $\bar{B}^0$ mesons in the data, and of the B meson lifetimes relative to the lifetime of the $\bar{B}^0$. The predicted number of lepton-charm used in the fit are expressed as

$$\begin{aligned} N(\ell^- D_i)_{predicted} &= \sum_{j=d,u,s} N(\bar{B}^0)\frac{f_j}{f_d} \times \tau(\bar{B}^0) \\ &\quad \times \tau(B_j)/\tau(\bar{B}^0) \sum_k \Gamma_k \times \mathcal{BR}_{ijk}(D_{jk} \to D_i)\mathcal{BR}(D_i)\epsilon_{ijk} \\ &= \sum_{j=d,u,s} N(\bar{B}^0)\frac{f_j}{f_u + f_d}\left(1 + \frac{f_u}{f_d}\right) \times \tau(\bar{B}^0) \\ &\quad \times \tau(B_j)/\tau(\bar{B}^0) \sum_k \Gamma_k \times \mathcal{BR}_{ijk}(D_{jk} \to D_i)\mathcal{BR}(D_i)\epsilon_{ijk} \end{aligned} \quad (9)$$

where $D_i = D^+, D^0, D^{*+}, D_s^+$ and $\Gamma_k = \Gamma, \Gamma^*, \Gamma^{**}$ for the meson case, and

$$N(\ell^- \Lambda_c^+)_{predicted} = N(\bar{B}^0)\frac{f_{\Lambda_b}}{f_u + f_d}\left(1 + \frac{f_u}{f_d}\right) \times \mathcal{BR}(\Lambda_b \to \ell^- \nu \Lambda_c^+ X)\epsilon(\Lambda_b^0 \to \ell^- \nu \Lambda_c^+ X) \quad (10)$$

for the baryon case. All of the Λ_b^0 and excited charm branching ratios in Equation (10) are included in the efficiency $\epsilon(\Lambda_b^0 \to \ell^- \nu \Lambda_c^+ X)$. There are four free parameters in the fit: three composition parameters f_u/f_d, $f_s/(f_u + f_d)$, $f_{\Lambda_b}/(f_u + f_d)$, termed $\{f_c\}$, and one normalization parameter $N(\bar{B}^0)$, and three constrained parameters: Γ, Γ^*, and Γ^{**}. f_s and f_{Λ_b} are fit relative to $f_u + f_d$ to minimize as many biases in the measurement as possible and to highlight the fact that the $\bar{B}_s^0$ is reconstructed relative to the $\bar{B}^0$ and B^- signals. Additionally, performing the fit relative to $f_u + f_d$ limits any possible inaccuracies in the separation of $\bar{B}^0$ and B^- through the sample composition into the $\ell^- D^0$ and $\ell^- D^+$ final states. The electron and muon samples are fit separately, since the relative lepton efficiencies between electrons and muons are not expected to readily cancel. The fit results for the e+SVT and μ+SVT data sets are given in in Table VI.

Fit Parameter	e+SVT	μ+SVT
f_u/f_d	1.044±0.028	1.062±0.024
$f_s/(f_u + f_d)$	0.162±0.008	0.158±0.006
$f_{\Lambda_b}/(f_u + f_d)$	0.292±0.020	0.275±0.015
Γ [ps^{-1}]	0.0157±0.0007	0.0154±0.0007
Γ^* [ps^{-1}]	0.0327±0.0014	0.0331±0.0013
Γ^{**} [ps^{-1}]	0.0145±0.0010	0.0146±0.0010
$N(\bar{B}^0)$ (10^9)	2.02±0.07	2.93±0.10

TABLE VI: Fit results *with statistical errors only.*

VI. SYSTEMATIC UNCERTAINTIES

The main source of systematic uncertainties in the measurement comes from the uncertainties in the branching ratios of the charm mesons, which contribute both directly and indirectly to the measurement, and the uncertainty associated with the baryon p_T spectrum, which affects the Monte Carlo efficiency. The uncertainties in the measurement due to

Systematic	f_u/f_d	$f_s/(f_u+f_d)$	$f_{\Lambda_b}/(f_u+f_d)$
WS	-0.039	-0.001	+0.018
Variation of cuts	±0.011	±0.0003	±0.019
D_s reflection	+0.001	+0.00002	+0.0001
XFT eff.	±0.003	±0.0004	±0.006
Single track	$^{+0.013}_{-0.014}$	±0.002	±0.002
Sample comp. lifetimes	$^{+0.018}_{-0.014}$	±0.006	±0.002
MC lifetimes	-	$^{+0.005}_{-0.001}$	$^{+0.0077}_{-0.0136}$
MC statistics	±0.005	±0.0007	±0.0006
p_T spectra	-	±0.008	±0.049
dE/dx eff.	-	-	±0.012
Λ_b^0 polarization	-	-	±0.007
Total (eff)	$^{+0.025}_{-0.045}$	$^{+0.011}_{-0.010}$	$^{+0.058}_{-0.056}$
$\mathcal{BR}(\Lambda_b^0 \to \ell^-\nu\Lambda_c^+ X)$	-	-	$^{+0.076}_{-0.048}$
Λ_b^0 sample composition	-	-	±0.045
$\mathcal{BR}(D^{**})$	±0.010	±0.004	±0.011
"physics bkgs"	±0.001	±0.002	±0.001
$\mathcal{BR}(D^+ \to K^-\pi^+\pi^+)$	±0.054	±0.003	±0.010
$\mathcal{BR}(D^0 \to K^-\pi^+)$	±0.020	±0.003	±0.003
$\mathcal{BR}(D_s^+ \to \phi\pi^+)$	±0.0006	$^{+0.057}_{-0.034}$	±0.001
$\mathcal{BR}(\Lambda_c^+ \to pK^-\pi^+)$	-	-	$^{+0.091}_{-0.053}$
Total ($\mathcal{BR}$)	±0.082	$^{+0.057}_{-0.034}$	$^{+0.128}_{-0.086}$
Total	$^{+0.086}_{-0.093}$	$^{+0.058}_{-0.035}$	$^{+0.141}_{-0.103}$

TABLE VII: Systematic uncertainties.

the particle species dependent trigger efficiencies and dE/dx efficiencies are negligible in comparison. The uncertainties assigned to the fragmentation fractions are listed in Table VII. The systematic uncertainties are determied the shift between a weighted average of the e+SVT and μ+SVT samples before and after the systematic variation.

The wrong sign (WS) systematic assigned accounts for possible fake leptons in the sample from wrong sign lepton-charm combinations, shown in Figure 7 for the μ+SVT data and Figure 8 where the width of the Gaussian fits to the WS combinations has been constrained to the width from the right sign lepton-charm signals, while the D_s^+ reflection uncertainty is assigned to the parameterization of the D_s^+ reflection which lies beneath the D^+ signal. The particle species dependent XFT trigger efficiencies are assigned to the knowledge of the differences in triggering for protons, kaons, and pions due to the energy loss of different particle species and the relatively tight trigger track requirement for hits in the drift chamber (COT). The single track efficiency has an uncertainty assigned due for the ability to determine the efficiency to add a track in Monte Carlo relative to data. The lifetimes which are used in the Monte Carlo generation affect the efficiencies and the lifetimes used in the sample composition to determine the B branching ratios also affect the fit result. Accurate knowledge of the $\bar{B}_s^0$ and Λ_b^0 p_T spectra are the biggest sources of systematic uncertainties assigned to efficiencies input in the sample composition for the measurement $f_s/(f_u+f_d)$ and $f_{\Lambda_b}/(f_u+f_d)$ respectively. The cuts applied to the charm signals are varied to determined the stability of the result and the difference is assigned as a systematic uncertaity. The uncertainties due to final state branching ratios are in all cases larger than those due to knowledge of the efficiencies of the decays.

VII. RESULTS

The weighted average of the fragmentation fractions between the electron plus displaced track and muon plus displaced track samples gives:

$$\begin{aligned}
\frac{f_u}{f_d} &= 1.054 \pm 0.018(stat)^{+0.025}_{-0.045}(sys) \pm 0.082(\mathcal{BR}) \\
\frac{f_s}{f_u+f_d} &= 0.160 \pm 0.005(stat)^{+0.011}_{-0.010}(sys)^{+0.057}_{-0.034}(\mathcal{BR}) \\
\frac{f_{\Lambda_b}}{f_u+f_d} &= 0.281 \pm 0.012(stat)^{+0.058}_{-0.056}(sys)^{+0.128}_{-0.086}(\mathcal{BR}).
\end{aligned}$$

This result is in agreement with the world averages of the fragmentation fraction of B^- relative to $\bar{B}^0$. The relative fragmentation fractions $f_s/(f_u + f_d)$ and $f_{\Lambda_b}/(f_u + f_d)$ differ from the world averages by $\sim 1\,\sigma$ and $\sim 2\,\sigma$ respectively. The central value of $f_{\Lambda_b}/(f_u + f_d)$ is higher than has previously been measured.

Extracting the poorly measured $\mathcal{BR}(D_s^+ \to \phi\pi^+)$ and $\mathcal{BR}(\Lambda_c^+ \to pK^-\pi^+)$ from the results for comparison with the world averages gives:

$$\begin{aligned}
\frac{f_s}{f_u + f_d} \times \mathcal{BR}(D_s^+ \to \phi\pi^+) &= (5.76 \pm 0.18(stat)^{+0.45}_{-0.42}(sys)) \times 10^{-3} \\
\frac{f_{\Lambda_b}}{f_u + f_d} \times \mathcal{BR}(\Lambda_c^+ \to pK^-\pi^+) &= (14.1 \pm 0.6(stat)^{+5.3}_{-4.4}(sys)) \times 10^{-3} \\
\frac{f_{\Lambda_b}}{f_u + f_d} \times \mathcal{BR}(\Lambda_b^0 \to \ell\nu\Lambda_c^+)\mathcal{BR}(\Lambda_c^+ \to pK^-\pi^+) &= (12.9 \pm 0.6(stat) \pm 3.4(sys)) \times 10^{-4}.
\end{aligned}$$

Acknowledgments

We thank the Fermilab staff and the technical staffs of the participating institutions for their vital contributions. This work was supported by the U.S. Department of Energy and National Science Foundation; the Italian Istituto Nazionale di Fisica Nucleare; the Ministry of Education, Culture, Sports, Science and Technology of Japan; the Natural Sciences and Engineering Research Council of Canada; the National Science Council of the Republic of China; the Swiss National Science Foundation; the A.P. Sloan Foundation; the Bundesministerium fuer Bildung und Forschung, Germany; the Korean Science and Engineering Foundation and the Korean Research Foundation; the Particle Physics and Astronomy Research Council and the Royal Society, UK; the Russian Foundation for Basic Research; the Comision Interministerial de Ciencia y Tecnologia, Spain; and in part by the European Community's Human Potential Programme under contract HPRN-CT-20002, Probe for New Physics.

---

[1] Charge conjugates are implied throughout the text.
[2] F. Abe *et al.*, The CDF Collaboration, Phys. Rev. D**54**, 6596 (1996);
F. Abe *et al.*, The CDF Collaboration, Phys. Rev. D**60**, 092005 (1999);
T. Affolder *et al.*, The CDF Collaboration, Phys. Rev. Lett. **84**, 1663 (2000).
[3] D. Buskulic *et al.*, ALEPH Collaboration, Phys. Lett. B**361**, 221 (1995);
P. Abreu *et al.*,DELPHI Collaboration, Phys. Lett. B**298**, 199 (1992);
P.D. Acton *et al.*,OPAL Collaboration, Phys Lett B**295**, 357 (1992).
[4] Heavy Flavor Averaging Group (HFAG), www.slac.stanford.edu/xorg/hfag/.
[5] S. Eidelman *et al.*, Particle Data Group, Phys. Lett. B**592**,1 (2004).
[6] D. Acosta *et al.*, The CDF Collaboration, Phys. Rev. D**71**, 032001 (2005).
[7] D.J. Lange, Nucl. Instrum. Meth. A**462**, 152 (2001).
[8] Shin-shan Yu (Pennsylvania U.),. FERMILAB-THESIS-2005-11, UMI-31-65771, UMI-31-65771-MC, 2005.

APPENDIX A: SAMPLE COMPOSITION

The B hadron decays included in the sample composition are given in Table VIII.

$\bar{B}^0$	B^-	$\bar{B}_s^0$	Λ_b^0
$\ell\nu D^+$	$\ell\nu D^0$	$\ell\nu D_s^+$	$\ell\nu\Lambda_c^+$
$\ell\nu D^{*+}$	$\ell\nu D^{*0}$	$\ell\nu D_s^{*+}$	$\ell\nu\Lambda_c(2593)^+$
$\to D^0\pi^+$	$\to D^0\pi^0/\gamma$	$\to D_s^+\gamma$	$\to \Sigma_c(2455)^{++}\pi^-$
$D^+\pi^0/\gamma$			$\hookrightarrow \Lambda_c^+\pi^+$
			$\to \Sigma_c(2455)^0\pi^+$
$\ell\nu D_1^+$	$\ell\nu D_1^0$	$\ell\nu D_{s1}^+(2460)$	$\hookrightarrow \Lambda_c^+\pi^-$
$\to D^{*0}\pi^+$	$\to D^{*0}\pi^0$	$\to D_{s0}^{*+}\pi^0$	$\to \Sigma_c(2455)^+\pi^0$
$\hookrightarrow D^0\pi^0/\gamma$	$\hookrightarrow D^0\pi^0/\gamma$	$\hookrightarrow D_s^+\pi^0$	$\hookrightarrow \Lambda_c^+\pi^0$
$\to D^{*+}\pi^0$	$\to D^{*+}\pi^-$	$\to D_s^+\gamma$	$\to \Lambda_c^+\pi^+\pi^-$
$\hookrightarrow D^0\pi^+$	$\hookrightarrow D^0\pi^+$		$\to \Lambda_c^+\pi^0\pi^0$
$D^+\pi^0/\gamma$	$D^+\pi^0/\gamma$		$\to \Lambda_c^+\gamma$
$\ell\nu D_0^{*+}$	$\ell\nu D_0^{*0}$	$\ell\nu D_{s0}^{*+}(2317)$	$\ell\nu\Lambda_c(2625)^+$
$\to D^0\pi^+$	$\to D^0\pi^0$	$\to D_s^+\pi^0$	$\to \Lambda_c^+\pi^+\pi^-$
$D^+\pi^0$	$D^+\pi^-$		$\to \Lambda_c^+\pi^0\pi^0$
			$\to \Lambda_c^+\gamma$
$\ell\nu D_1^{'+}$	$\ell\nu D_1^{'0}$	$\ell\nu D_{s1}^{'+}(2535)$	
$\to D^{*0}\pi^+$	$\to D^{*0}\pi^0$	$\to D^{*+}K^0$	$\ell\nu\Sigma_c(2455)^{++}\pi^-)$
$\hookrightarrow D^0\pi^0/\gamma$	$\hookrightarrow D^0\pi^0/\gamma$	$\hookrightarrow D^0\pi^+$	$\to \Lambda_c^+\pi^+$
$\to D^{*+}\pi^0$	$\to D^{*+}\pi^-$	$D^+\pi^0/\gamma$	
$\hookrightarrow D^0\pi^+$	$\hookrightarrow D^0\pi^+$	$\to D^{*0}K^+$	$\ell\nu\Sigma_c(2455)^0\pi^+$
$D^+\pi^0/\gamma$	$D^+\pi^0/\gamma$	$\hookrightarrow D^0\pi^0/\gamma$	$\to \Lambda_c^+\pi^-$
$\ell\nu D_2^{*+}$	$\ell\nu D_2^{*0}$	$\ell\nu D_{s2}^{'+}(2573)$	$\ell\nu\Sigma_c(2455)^+\pi^0$
$\to D^{*0}\pi^+$	$\to D^{*0}\pi^0$	$\to D^{*+}K^0$	$\to \Lambda_c^+\pi^0$
$\hookrightarrow D^0\pi^0/\gamma$	$\hookrightarrow D^0\pi^0/\gamma$	$\hookrightarrow D^0\pi^+$	
$\to D^{*+}\pi^0$	$\to D^{*+}\pi^-$	$D^+\pi^0/\gamma$	$\ell\nu\Lambda_c^+ f_0$
$\hookrightarrow D^0\pi^+$	$\hookrightarrow D^0\pi^+$	$\to D^{*0}K^+$	
$D^+\pi^0/\gamma$	$D^+\pi^0/\gamma$	$\hookrightarrow D^0\pi^0/\gamma$	$\ell\nu\Lambda_c^+\pi^+\pi^-$(NR)
$\to D^0\pi^0$	$\to D^0\pi^0$	$\to D^+K^0$	
$\to D^+\pi^-$	$\to D^+\pi^-$	$\to D^0K^+$	$\ell\nu\Lambda_c^+\pi^0\pi^0$(NR)
$\ell\nu D^{*+}\pi^0$(NR)	$\ell\nu D^{*+}\pi^-$(NR)	$\ell\nu D_s^{*+}\pi^0$(NR)	
$\to D^0\pi^+$	$\to D^0\pi^+$	$\to D_s^+\gamma$	
$D^+\pi^0/\gamma$	$D^+\pi^0/\gamma$		
		$\ell\nu D_s^+\pi^0$(NR)	
$\ell\nu D^{*0}\pi^+$(NR)	$\ell\nu D^{*0}\pi^0$(NR)		
$\to D^0\pi^0/\gamma$	$\to D^0\pi^0/\gamma$		
$\ell\nu D^+\pi^0$(NR)	$\ell\nu D^+\pi^-$(NR)		
$\ell\nu D^0\pi^+$(NR)	$\ell\nu D^0\pi^0$(NR)		
$D^{(*)}\bar{D}^{(*)}K$	$D^{(*)}\bar{D}^{(*)}K$	$D^{(*)}\bar{D}^{(*)}K$	
$D^{(*)+}D^{(*)-}$			
$D_s^{(*)}D^{(*)}X$	$D_s^{(*)}D^{(*)}X$	$D_s^{(*)}D^{(*)}X$	$\tau^-\nu\Lambda_c^+$
		$D_s^{(*)}D_s^{(*)}X$	$\tau^-\nu\Lambda_c(2593)^+$
$\tau^-\nu D^{+(*),(**)}$	$\tau^-\nu D^{0(*),(**)}$	$\tau^-\nu D_s^{+(*),(**)}$	$\tau^-\nu\Lambda_c(2625)^+$

TABLE VIII: $\bar{B}$ hadron sample composition.

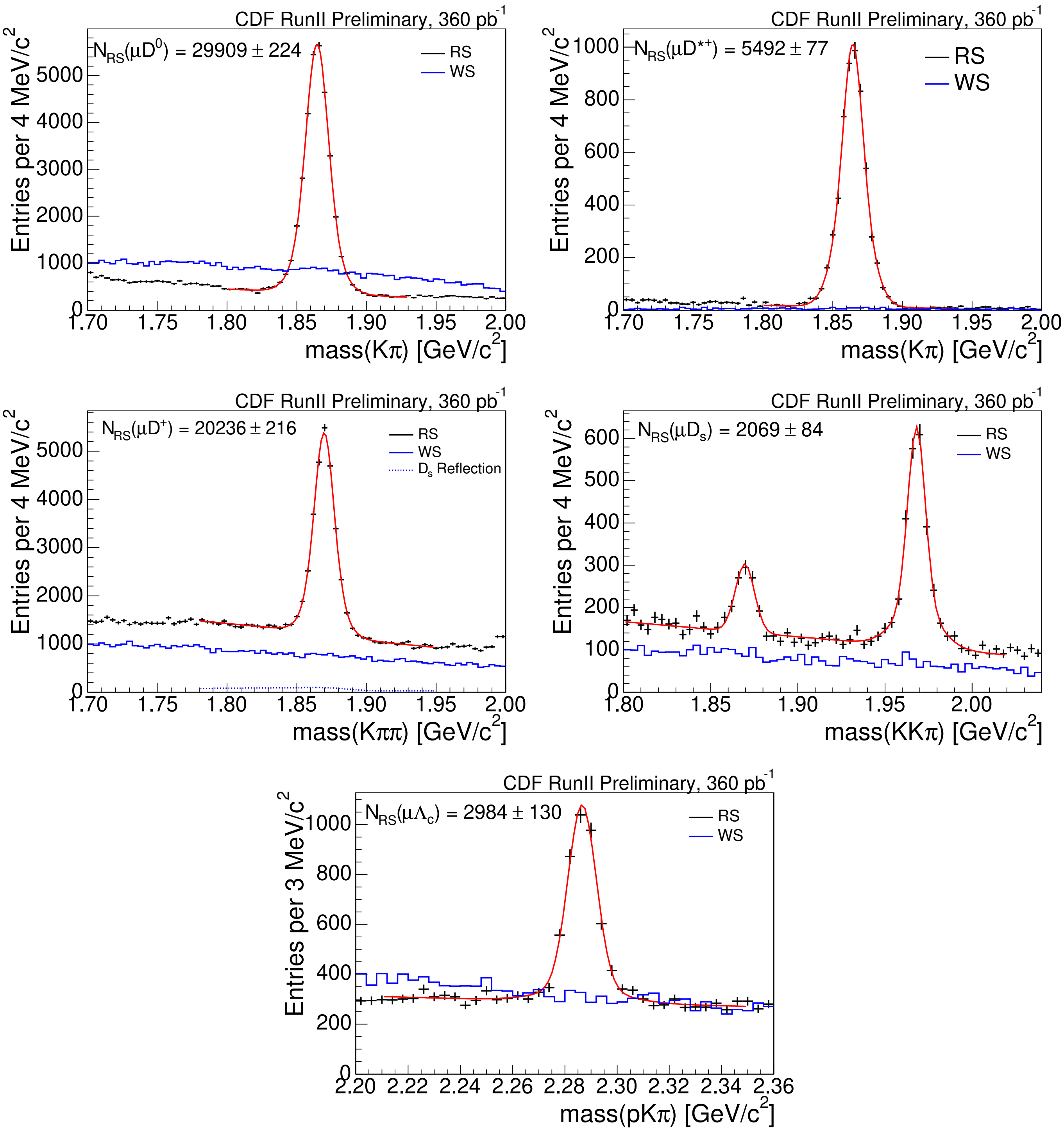

FIG. 1: μ+SVT right sign (black) and wrong sign (blue) invariant mass distribution of D^0 (top left), D^{*+} (top right), D^+ (middle left), D_s^+ (middle right), Λ_c^+ (bottom) with all analysis cuts applied.

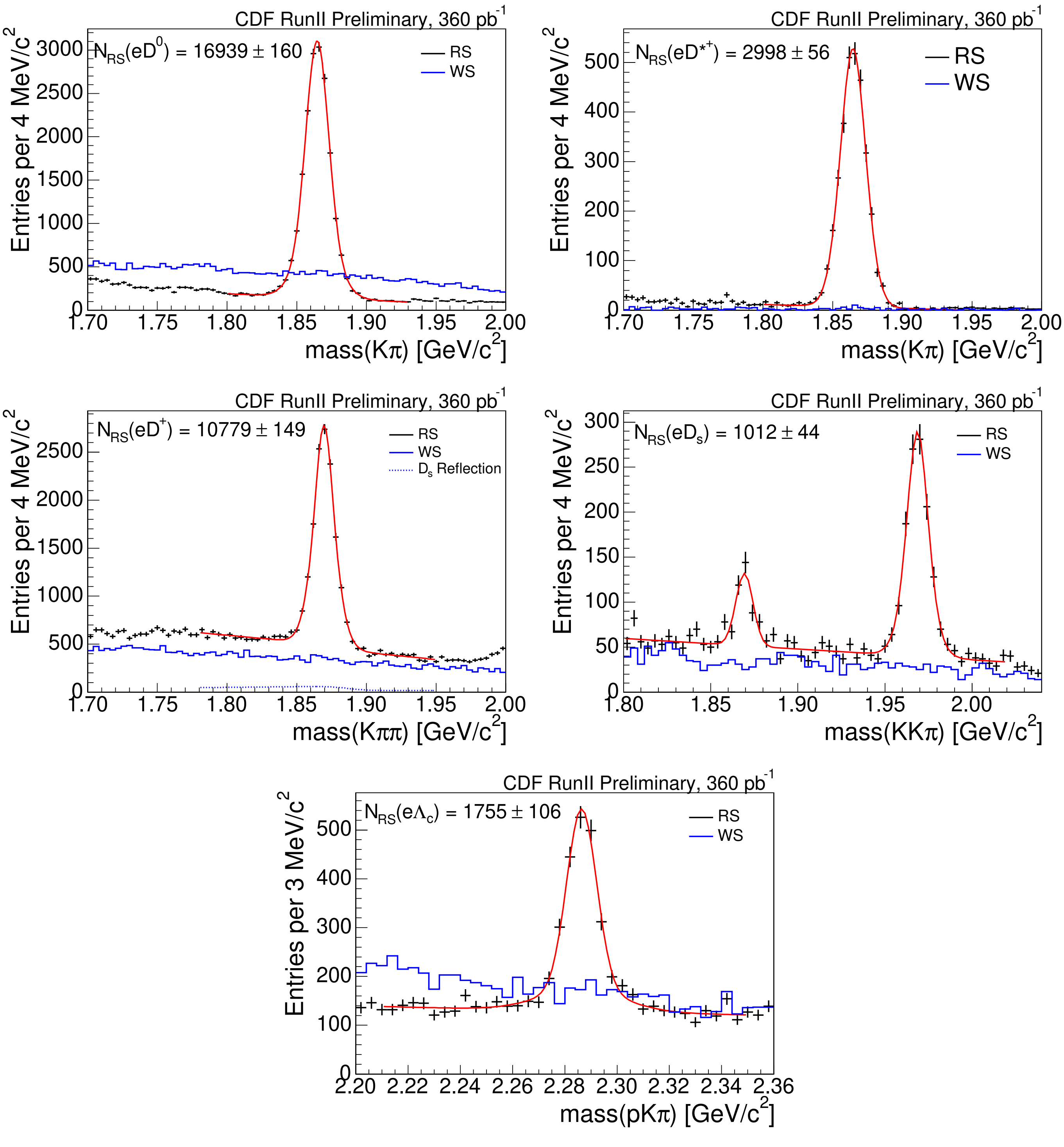

FIG. 2: e+SVT right sign (black) and wrong sign (blue) invariant mass distribution of D^0 (top left), D^{*+} (top right), D^+ (middle left), D_s^+ (middle right), Λ_c^+ (bottom) with all analysis cuts applied and fit parameterizations overlaid.

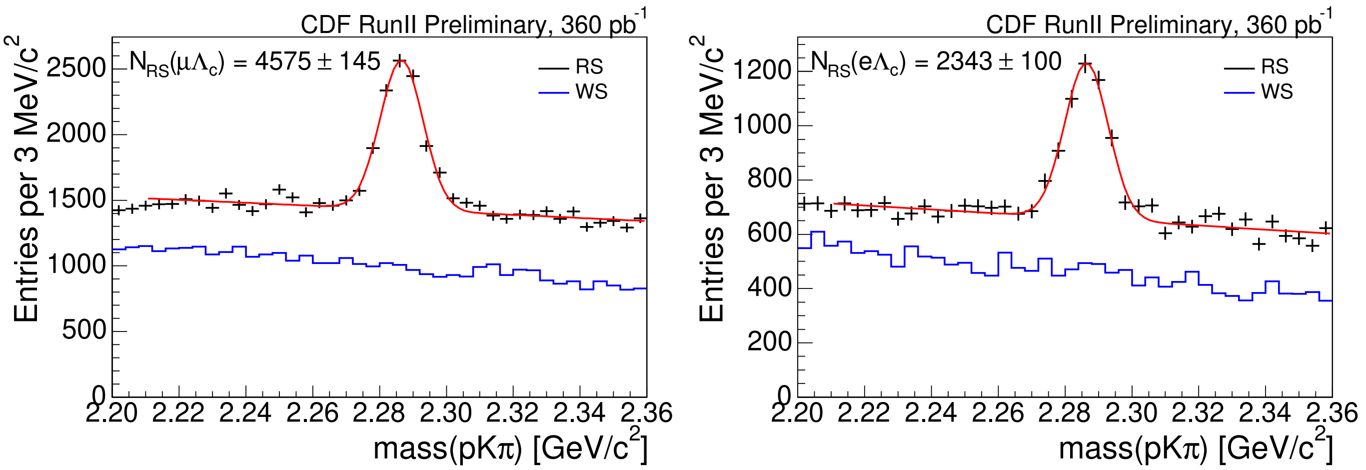

FIG. 3: Λ_c^+ signals without the dE/dx cut applied for the μ+SVT data (left) and e+SVT data (right).

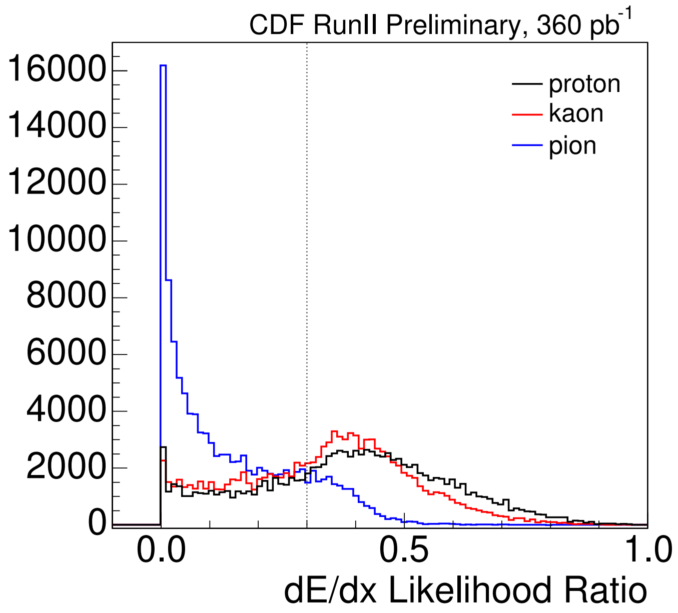

FIG. 4: dE/dx $\mathcal{LR}$ distribution with the proton mass hypothesis. The proton comes from $\Lambda \to p\pi$, while the kaon and pion come from $D^{*+} \to [K\pi]\pi$. The cut value is shown with the dashed line.

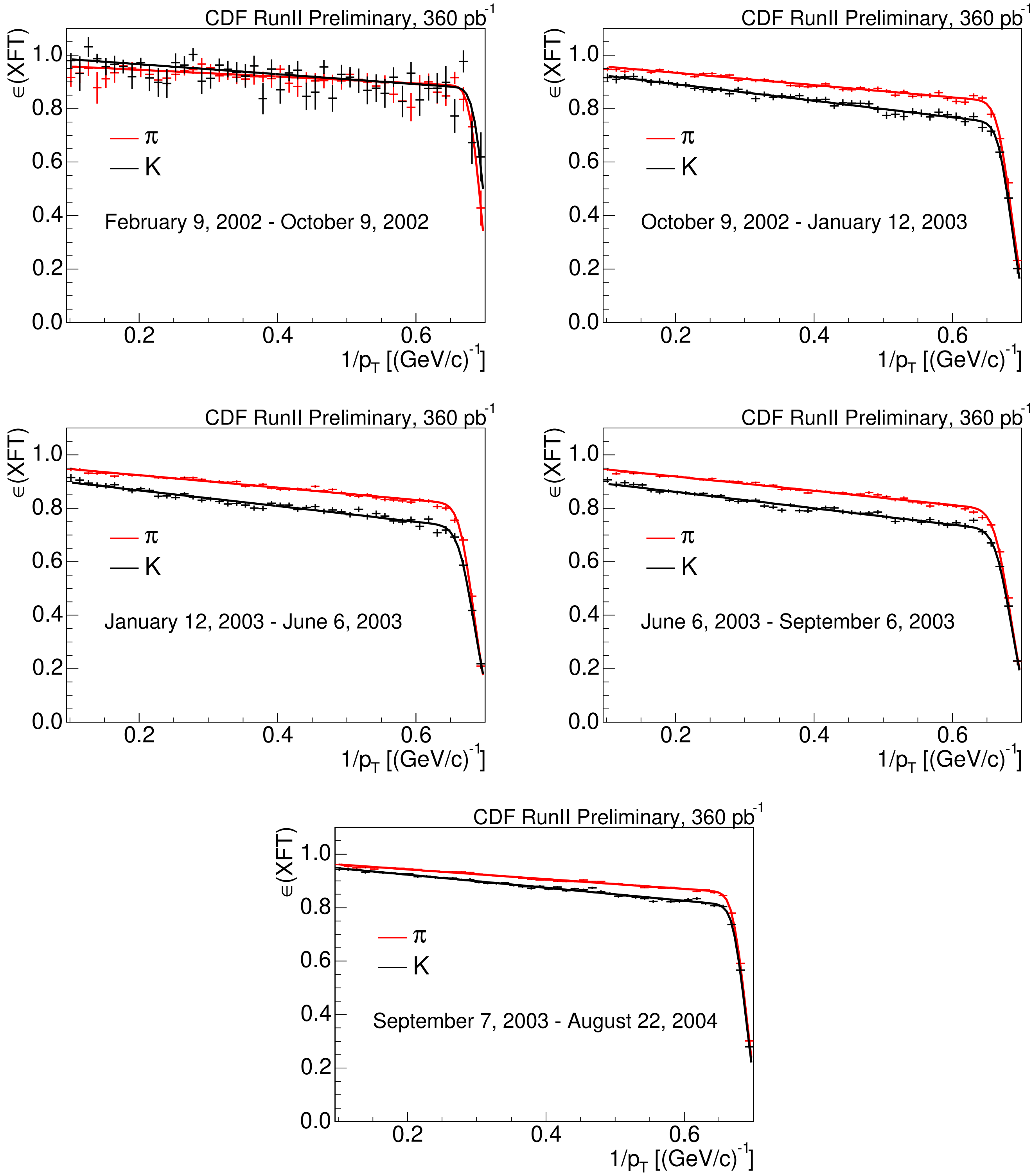

FIG. 5: ϵ_{XFT} as a function of p_T^{-1} for pions (red) and kaons (black) for various run ranges indicated.

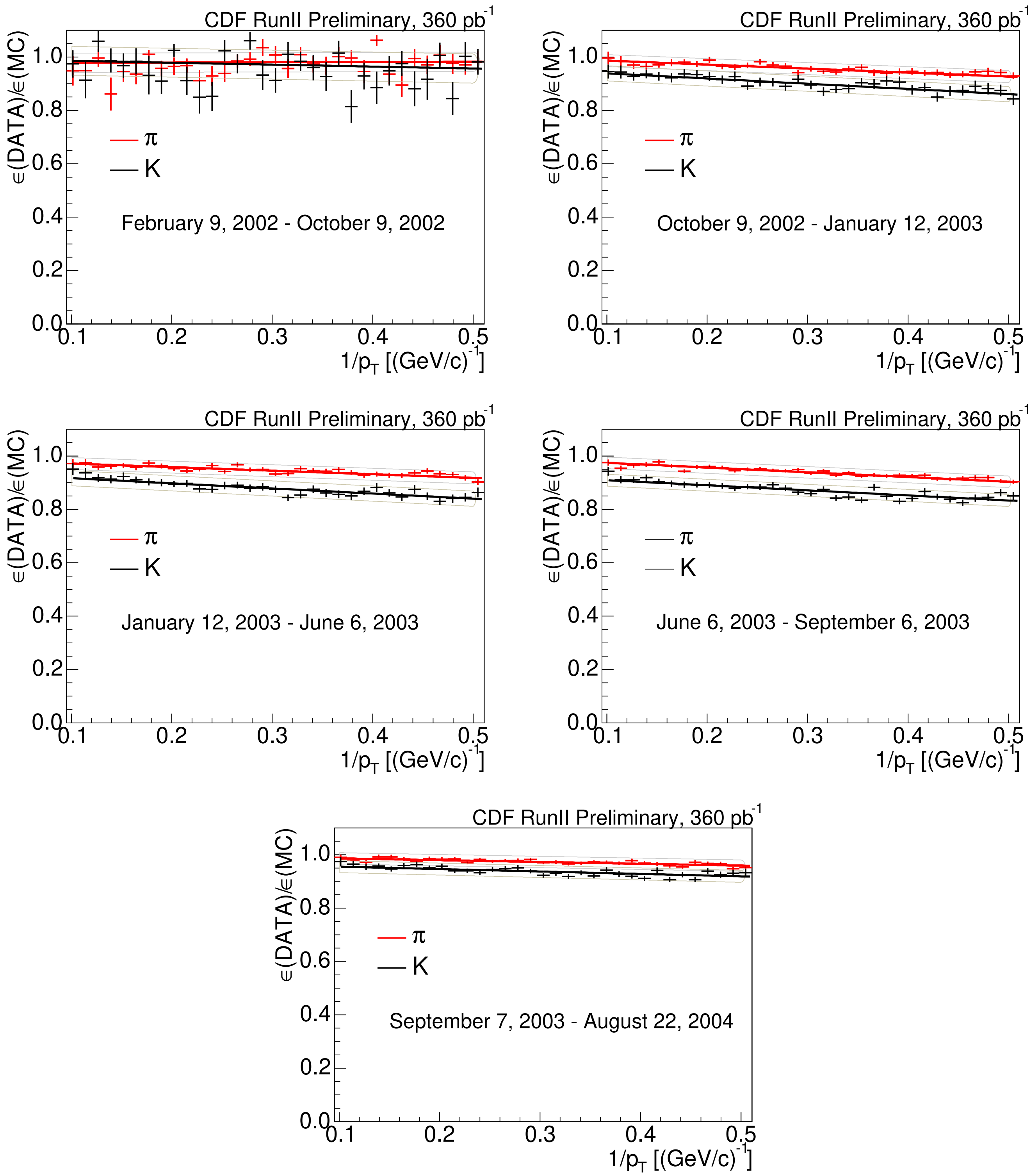

FIG. 6: $\epsilon_{XFT}(DATA)/\epsilon_{XFT}(MC)$ as a function of p_T^{-1} for pions (red) and kaons (black).

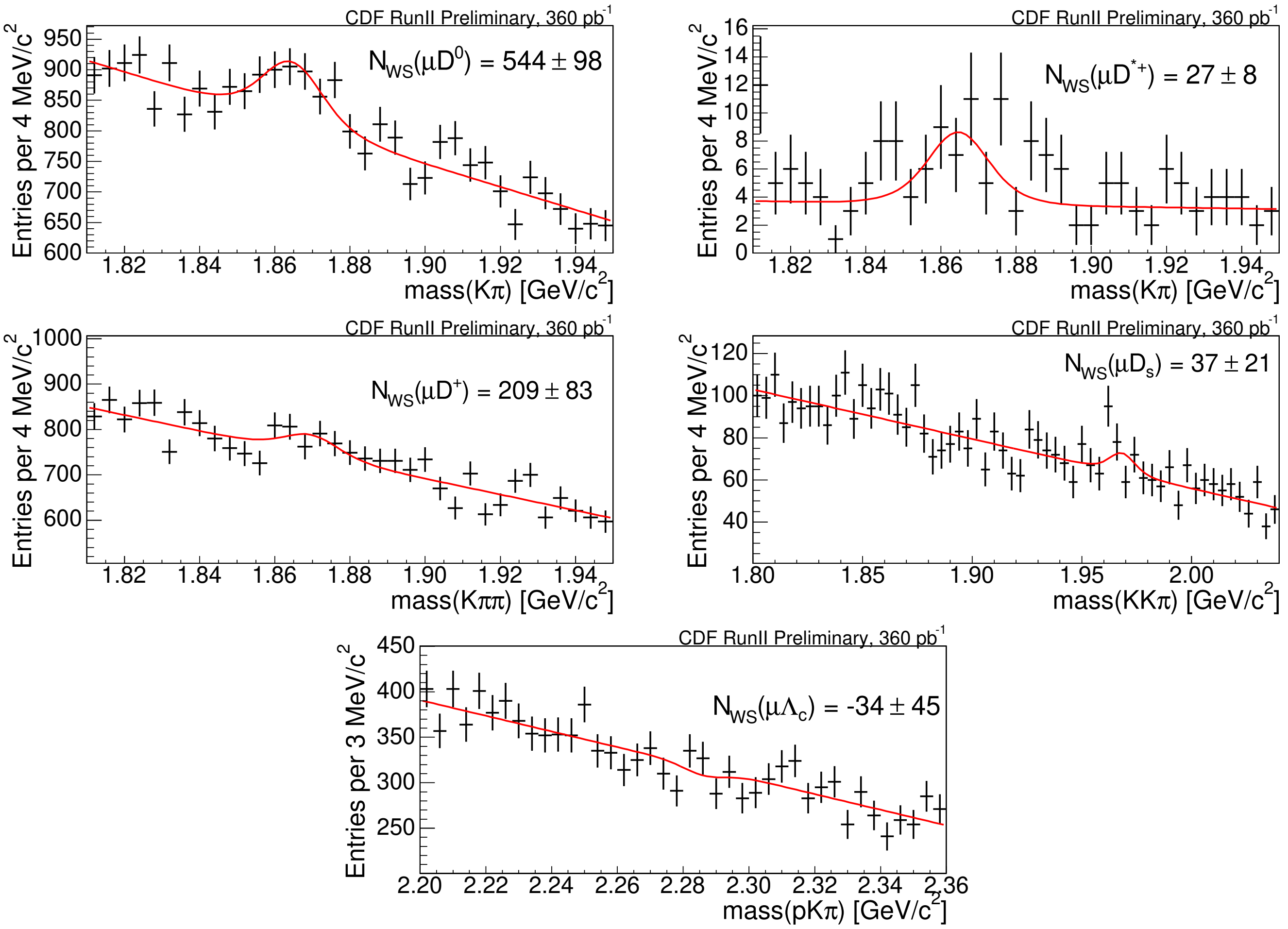

FIG. 7: μ+SVT wrong sign invariant mass distributions of (top to bottom, left to right) D^0, D^{*+}, D^+, D_s^+, and Λ_c^+ after the $ct^*(B)$ cut.

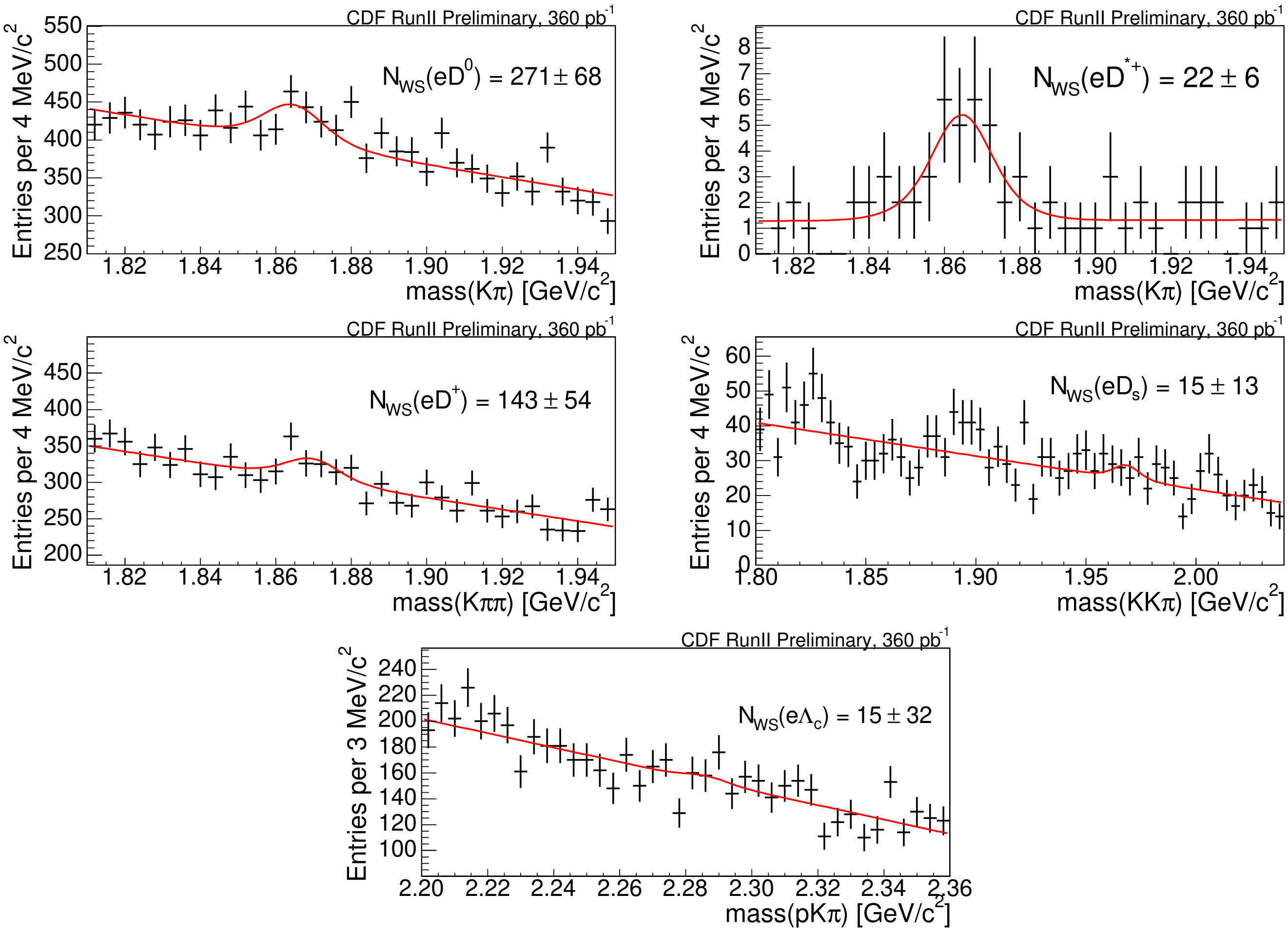

FIG. 8: e+SVT wrong sign invariant mass distributions of (top to bottom, left to right) D^0, D^{*+}, D^+, D_s, and Λ_c after the $ct^*(B)$ cut.